# The Developing Left Superior Cervical Ganglion of Pacas *(Agouti Paca)*

**SAMANTA RIOS MELO,[1] JENS RANDEL NYENGAARD,[2] FELIPE DA ROZA OLIVEIRA,[1] FERNANDO VAGNER LOBO LADD,[1] LUCIANA MARIA BIGARAM ABRAHÃO,[1] MÁRCIA R.F. MACHADO,[3] TAIS H.C. SASAHARA,[1] MARIANA PEREIRA DE MELO,[4] AND ANTONIO AUGUSTO C.M. RIBEIRO[1*]**

[1]Laboratory of Stochastic Stereology and Chemical Anatomy (LSSCA), Department of Surgery, College of Veterinary Medicine, University of São Paulo (USP), São Paulo, Brazil
[2]Stereology and Electron Microscopy Research Laboratory and Mind Centre, University of Aarhus, 8000, Aarhus, Denmark
[3]Department of Morphology and Physiology, College of Veterinary Medicine, São Paulo State University (UNESP), Jaboticabal, São Paulo, Brazil
[4]Department of Statistics, Institute of Mathematics and Statistics, University of São Paulo, Brazil

ABSTRACT

In this study the main question investigated was the number and size of both binucleate and mononucleate superior cervical ganglion (SCG) neurons and, whether post-natal development would affect these parameters. Twenty left SCGs from 20 male pacas were used. Four different ages were investigated, that is newborn (4 days), young (45 days), adult (2 years), and aged animals (7 years). By using design-based stereological methods, that is the Cavalieri principle and a physical disector combined with serial sectioning, the total volume of ganglion and total number of mononucleate and binucleate neurons were estimated. Furthermore, the mean perikaryal (somal) volume of mononucleate and binucleate neurons was estimated using the vertical nucleator. The main findings of this study were a 154% increase in the SCG volume, a 95% increase in the total number of mononucleate SCG neurons and a 50% increase in the total volume of SCG neurons. In conclusion, apart from neuron number, different adaptive mechanisms may coexist in the autonomic nervous system to guarantee a functional homeostasis during ageing, which is not always associated with neuron losses. Anat Rec, 292:966–975, 2009. © 2009 Wiley-Liss, Inc.

**Key words: SCG; stereology; physical disector; ageing; pacas**

Post-natal development comprises both maturation (from newborn to adult) and ageing (from adult to senility) and, during this phase, several adaptive organic mechanisms occur, albeit they are not fully understood (Finch, 1993; Vega et al., 1993). For instance, the final number of neurons is established during fetal life, but mitosis can be found in rats after birth. Moreover, in the first week of life, the number of neurons remains unchanged or shows a small decrease (Erankö, 1972). Nevertheless, these claims are controversial because there are differences between various components of the nervous system, and between animal species (Finch, 1993; Vega et al., 1993).

Grant sponsor: FAPESP; Grant number: 04/15882-0; Grant sponsor: Lundbeck Foundation.

*Correspondence to: Antonio Augusto C.M. Ribeiro, Departamento de Cirurgia, Faculdade de Medicina Veterinária e Zootecnia, Universidade de São Paulo, Av. Prof. Dr. Orlando Marques de Paiva, 87- CEP 05508-270, São Paulo –SP, Brazil. Fax: 55 11 3032 2224. E-mail: guto@usp.br

Received 30 April 2008; Accepted 23 March 2009

DOI 10.1002/ar.20918
Published online 28 May 2009 in Wiley InterScience (www.interscience.wiley.com).

Fig. 1. Details of two adult (2-year-old) pacas (*Agouti paca*) weighing about 12 kg. In captivity, the animal lifespan is up to 16 years.

The number of neurons in the hypogastric ganglion of 24-month-old rats of is higher than in 4-month-old rats (Warburton and Santer, 1997), and it is higher in the dorsal root ganglia (DRG) of 80-day-old rats than in 11-day-old rats (Popken and Farel, 1997). In addition, Farel (2003) reported that the increase in the number of neurons in the rat's DRG was not associated with a possible neurogenesis, but perhaps with a late maturation or incomplete differentiation. Because binucleate superior cervical ganglion (SCG) neurons have been described in adult wild rodents such as capybaras (Ribeiro et al., 2004; Ribeiro, 2006), and lagomorphs (rabbits) (Sasahara et al., 2003), there is a need for conclusive studies on a possible neurogenesis after birth.

Given the findings above, this article aimed at investigating whether maturation and ageing would affect the number and size of binucleate and mononucleate SCG neurons in wild rodents lighter than capybaras and, therefore, more related to rats and guinea pigs, which are currently being investigated (Purves et al., 1986b).

Pacas are wild rodents, the males of which weigh up to around 12 kg and have a lifespan of 12–13 years in the wild, and up to 16 years in captivity (Fig. 1) (Nowak, 1999). Pacas were chosen since there are few data available about these animals. As a consequence, there is an increased interest in multidisciplinary studies on the developmental biology of this species aimed at better breeding and preserving this second biggest Brazilian rodent, which is at risk and is very important in terms of meat consumption in Brazil (Rowe and Honeycutt, 2002; Wilson and Reeder, 2005). Additionally, pacas are more allometrically related to humans, which may turn this species into a suitable model for understanding postnatal on-going changes in mammalian autonomic ganglia.

## MATERIALS AND METHODS

### Materials

Twenty left SCG from 20 male pacas (*Agouti paca*) were obtained from the animal facility of São Paulo State University (UNESP), Jaboticabal, São Paulo, Brazil which is licensed by the Brazilian Ministry of Environment (IBAMA) (License number is 1-35-92-0882-5). The animals were divided into four age groups with five animals in each; Group 1: newborn (four-day-old, mean body weight: 862 g), Group 2: young (45-day-old, mean body weight: 1.81 kg), Group 3: adult (2-year-old, mean body weight: 6.85 kg) and Group 4: aged (7-year-old, mean body weight: 8.79 kg).

### Methods

Animals were sedated with azaperone (4 mg/kg/IM) followed by atropine sulphate (0.06 mg/kg/IM). For the anesthesia, a combination of ketamine chloride (20 mg/kg/IM) and xylazine hydrochloride (1.5 mg/kg/IM) (Bayer®) was administered and the euthanasia procedure was conducted using an overdose of thionembutal (100 mg/kg/IV). A bulbed cannula was inserted into the left ventricle and a solution of phosphate-buffered saline (PBS; Sigma®; 0.1 M; pH 7.4) containing 2% of heparin (Roche®) and 0.1% of sodium nitrite (Sigma®) was perfused through the ascending aorta, and it was followed by a modified Karnovsky solution (3% glutaraldehyde and 1% formaldehyde) in sodium cacodylate buffer (EMS®; 0.125 M; pH 7.4). The left SCGs were then dissected out and their thickness, width and length were measured using a digital pachymeter (Digimess®).

Subsequently, the SCGs' wet weights were converted into volumes to estimate the tissue shrinkage using a tissue density of 1.06 g/cm$^3$. The latter was estimated in three left SCGs per age group in a pilot study by simply weighing the SCGs and dividing their wet weights (g) (after perfusion-fixation) by their volumes (cm$^3$) estimated by liquid displacement (Scherle, 1970). Mean tissue densities and their coefficients of variation (CVs) were 1.059 g/cm$^3$ (0.01) (newborn), 1.061 g/cm$^3$ (0.01) (young), 1.060 g/cm$^3$ (0.01) (adult), and 1.061 g/cm$^3$ (0.01) (aged) pacas. Since intergroup differences did not attain significance ($P = 0.44$), the same tissue density, that is 1.06 g/cm$^3$, was used for all age groups to estimate tissue shrinkage (See volume of ganglion, V(SCG), for methodological details).

To produce vertical and uniform random sections (VUR sections) (Baddeley et al., 1986; Tandrup, 1993; Tandrup and Braendgaard, 1994) the whole ganglion was randomly rotated along their longitudinal axis (ganglion length) using a bar rotator. After rotation, the vertical axis was, therefore, marked using a Tissue Marking Dye System (Cancer Diagnostics, INC®) (Fig. 2).

Subsequently, SCGs were embedded in a 7% agar solution, and using a tissue slicer, they were systematically, uniformly and randomly cut into 1-mm thick slabs (with a random start between 0 and 1 mm) and generating four, five, and seven slabs in newborn, young, adult, and aged pacas, respectively. Next step, each slab was placed onto a horizontal plane and manually halved with a scalpel along a cutting line, that is a line which divided each ganglion slab into two almost-equal-sized half-slabs to fit into araldite-embedding mould dimensions. The halving was, therefore, performed perpendicularly to the horizontal plane containing the slabs, producing on average eight, 10, and 14 tissue blocks in newborn, young, adult, and aged pacas, respectively (Fig. 2). This design is similar to the one employed by Tandrup (1993) to unbiasedly and efficiently estimate number and mean volume of

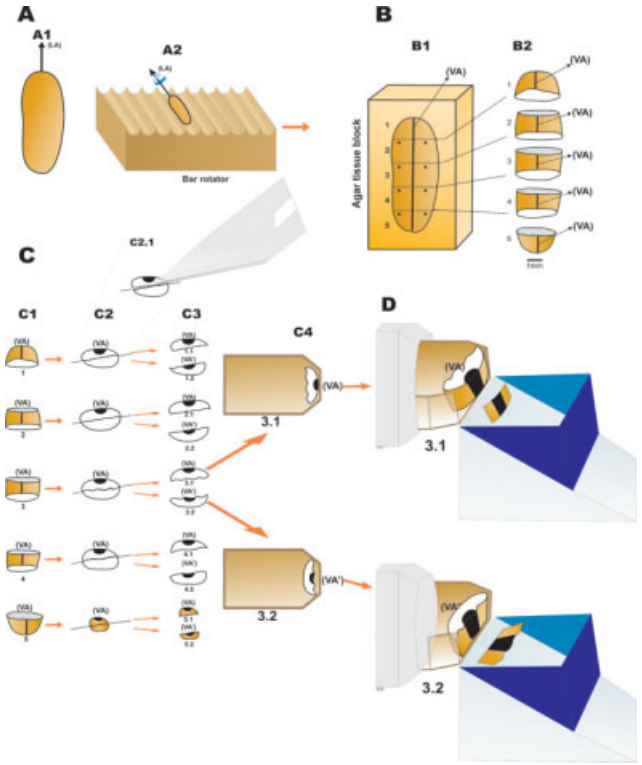


Fig. 2. Schematic drawing of SCG (A1), which was clockwise rotated (orientation arrow) along its longitudinal axis (LA) using a bar rotator (A2). After rotation, the vertical axis (VA) was, therefore, marked on the SCG, which was subsequently agar-embedded (B1) and SUR sliced (B2) into five 1-mm slabs. Subsequently each slab (C1) was placed onto a horizontal plane and manually halved with a scalpel along a crooked cutting line (C2 and C2.1), that is a line produced with the use of a scalpel, which divides each ganglion slab into two almost-equal-sized half-slabs to fit into the araldite-embedding mould dimensions (C4). This procedure gave risen to ten tissue blocks (from 1.1 to 5.2) (C3), which were araldite-embedded (C4). Next, VUR sections where cut from these araldite blocks with glass knives (D), collected onto glass slides, stained with toluidine blue, and mounted under coverslips. Note that in the example given, block 3.2 was cut after block 3.1, and keeping the same sectioning direction used for cutting block 3.1 (VA), which is actually the vertical axis. For didactic reasons, in block 3.2, the sectioning direction was represented by (VA′) which is parallel to VA. By analogy, the same notation (VA′) was adopted for block 1.2 cut after block 1.1; block 2.2 cut after block 2.1; block 4.2 cut after block 4.1, and block 5.2 cut after block 5.1 (see C3). Scale bar: 1 mm.

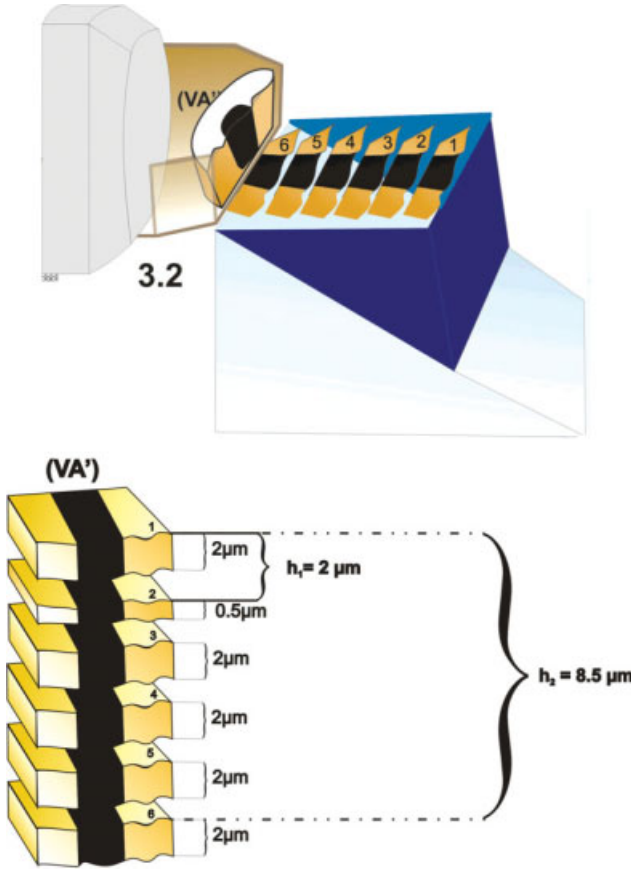


Fig. 3. Schematic drawing depicting a set of sections cut from araldite block 3.2 (see Fig. 2) used for illustrating the modified physical disector used. Each set of sections comprised six consecutive sections, that is one 2-µm thick section (reference-section) followed by another 0.5-µm thick section (look-up 1 section; the smaller physical disector height was 2 µm), and four more 2-µm thick sections. The last of these four 2-µm thick sections was the look-up 2 section (the larger physical disector height was 8.5 µm).

dorsal root ganglion (DRG) neurons of rats. The DRG was longitudinally sectioned into two equal-sized halves, which were embedded in the same glycolmethacrylate-embedding mould due to the small size of the ganglion (2 mm long and 1 mm in diameter) (Tandrup, 1993). However, in the case of paca SCG, which was up to 7.66 mm in length (see Results section), each half-slab of a ganglion slab was embedded in one araldite-embedding mould, and they were cut one after the other (Fig. 2).

Later on, all tissue blocks were washed in sodium cacodylate buffer, post-fixed in a solution of 2% osmium tetroxide in sodium cacodylate buffer, stained en bloc with a saturated aqueous solution of uranyl acetate (EMS®), dehydrated in graded ethanol concentrations and propylene oxide (EMS®) and embedded in Araldite 502 (EMS®). Araldite blocks were polymerized in the oven at 60–70°C for three days. For light microscopy, 0.5 and 2-µm thick sections were cut with glass knives using a Leica® UC6 calibrated ultramicrotome. Subsequently, sections were collected onto glass slides, dried on a hot plate, stained with toluidine blue, and mounted under a coverslip with a drop of Araldite (Fig. 2). Section images were acquired using a DMR Leica® microscope equipped with a DFC 300 FX Leica® digital camera and projected onto a computer monitor. Image analysis was performed on a flat computer screen, using a QWin V3 Leica® morphometric software. It has to be stressed that the identification of binucleate neurons was based upon counting the total number of nuclei per neuron using serial sections, and not only in a single section.

***Stereology (design-based).*** A modification of the disector (Gundersen, 1986) and later demonstrated by (Eskild-Jensen et al., 2007) was used in this study. Our approach comprised reference and two look-up sections and, therefore two disector heights, including a stack of serial sections between them (Fig. 3). Such procedure

was used in this study in order to ascertain a correct identification and sampling of mononucleate and binucleate neurons in semi-thin sections for light microscopy.

***Numerical density of mononucleate and binucleate neurons: $N_v$ (mononuc, SCG) and $N_v$ (binuc, SCG).*** The modified physical disector was used to estimate the numerical density. The method consists of counting the number of neurons that are present within unbiased counting frames on reference sections, which do not touch either the forbidden lines of the frames or their extensions and disappear on parallel look-up sections.

The optical disector was not used since we did not have stereological software for implementing the optical counting at that time. Furthermore, we took advantage of broader expertise in applying the physical disector to semi-thin araldite sections of sympathetic ganglia of medium-sized and large mammals (Ribeiro et al., 2004; Gagliardo et al., 2005; Ribeiro, 2006).

The formula for $N_v$ estimation is: $N_V$: = $\Sigma Q^-$(SCG cell)/$\Sigma$V(SCG) where $\Sigma Q^-$ represents the cell count and $\Sigma$V(SCG) is the volume of all disectors sampled. The latter is estimated as $\Sigma P \cdot (a/p) \cdot h$, where $P$ is the number of test points, $(a/p)$ the area associated with each test point and h the distance between disector planes (disector height). Unbiased counting frames (frame area = 89,100 $\mu m^2$) (Gundersen, 1977) were SUR superimposed on section fields of view and the same sampled area was followed toward six consecutive sections, that is one 2-μm thick section followed by another 0.5-μm thick section and four more 2-μm thick sections (Fig. 3). Disectors were SUR applied (every 150th section) along the whole SCG length, that is in all SCG slabs (Gundersen et al., 1999). Cell nucleoli were used as the counting unit for estimating cell volume (see mean volume of mononucleate and binucleate neurons) using the small physical disector with the first look-up section being 2 μm distant from the reference section, that is the smaller disector height was 2 μm. Additionally, the perikarya (soma) were used as the counting unit for estimating the total number of SCG neurons using the larger physical disector with the second look-up section (the larger disector height was 8.5 μm) (Fig. 3).

For mononucleate neurons, on an average 76 disectors were used to count 109 cells in newborn, 44 disectors to count 105 cells in young, 46 disectors to count 102 cells in adult and 56 disectors to count 104 cells in aged pacas. The mean number of disectors applied per SCG slab was 19, 8, 6, and 8 in newborn, young, adult, and aged pacas, respectively.

For binucleate neurons, on average 80 disectors were used to count 100 cells in newborn, 64 disectors to count 105 cells in young, 90 disectors to count 103 cells in adult, and 94 disectors to count 103 cells in aged pacas. The mean number of disectors applied per SCG slab was 20, 12, 12, and 13 in newborn, young, adult, and aged pacas, respectively.

To estimate the numerical density of SCG mono and binucleate neurons on average 15, 17, 24, and 25 sets of sections were used for newborn, young, adult, and aged pacas, respectively.

### Volume of Ganglion: V(SCG)

The total volume of SCG was estimated by means of the Cavalieri principle. Briefly, SCG Araldite-embedded blocks were exhaustively and serially sectioned and every 300th section ($K = 300$) was sampled, with a random start between 0 and 300, and measured for cross-sectional area. The volume estimation was performed in a fraction (Fn = 1/2) of the reference sections used for neuron numerical density estimation, that is on an average 8, 10, 14, and 14 sections for newborn, young, adult, and aged pacas, respectively. Then, V(SCG): = $T \cdot \Sigma A$, where $T$ is the intersectional distance = 600 μm, $\Sigma A$ is the sum of delineated areas of the SCGs, which were calculated using test points hitting the whole reference space ($P \sim 200$ in newborn and young pacas and ~250 in adult and aged pacas). Shrinkage volume (%) was estimated to be (mean ± SD): newborn: 8.75 ± 1.23, young: 7.56 ± 1.51, adult: 7.16 ± 1.31, and 7.05 ± 1.37 for aged pacas. No correction for global shrinkage was performed since intergroup differences were not statistically significant ($P = 0.4$).

***Total number of mononucleate and binucleate neurons: N(mononuc, SCG) and N(binuc, SCG).*** The total number of SCG neurons (both mononucleate and binucleate) was estimated by multiplying $N_V$ by SCG volume: $N = N_V \cdot V$.

### Volume Density of Neurons: $V_v$(neurons, SCG) and of the Non-Neuronal Tissue: Neuropil ($V_v$(neuropil, SCG)) and Capillaries ($V_v$(cap, SCG))

The fractional volume of SCG occupied by neurons (perikaryon or soma) and the one occupied by neuropil and capillaries was estimated by point counting in the same sections and employing the same number of points ($P$) used for the Cavalieri estimate, that is on an average 8, 10, 14, and 14 sections for newborn, young, adult, and aged pacas, respectively, and $P \sim 200$ for newborn and young and ~250 for adult and aged pacas (Fig. 4).

A SUR sampling of fields was elicited and test points were randomly superimposed on a computer monitor. We counted the total number of points falling within the SCG $\Sigma$P(SCG) and the total number of points falling on neurons, neuropil, and capillaries ($\Sigma$P(SCG) neurons, neuropil, cap). Volume density was therefore estimated as: $V_V$: = $\Sigma$P(SCG) neurons, neuropil, cap : $\Sigma$P(SCG).

### Total Volume of Neurons: V(neurons, SCG) and of the Non-Neuronal Tissue: Neuropil (V(neuropil, SCG)) and Capillaries (V(cap, SCG))

The total volume occupied by neurons (perikaryon or soma) and occupied by neuropil and capillaries was indirectly estimated by multiplying their fractional volumes by the total volume of SCG, V(SCG) (Lima et al., 2007).

### Mean Volume of Mononucleate and Binucleate Neurons: $\overline{v}_N$(mononuc, SCG) and $\overline{v}_N$(binuc, SCG)

The mean perikaryal (somal) volume of both mono and binucleate neurons was estimated by the Nucleator

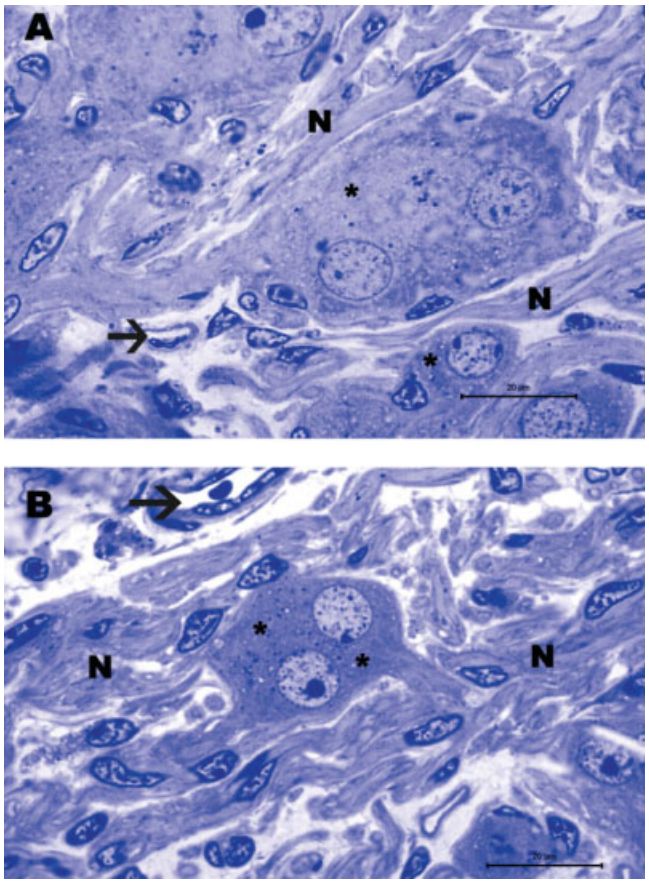


Fig. 4. Fine structure of the superior cervical ganglion of an adult paca (**A, B**), in semi-thin sections (2 μm) at the same magnification, depicting the three distinct ganglion compartments used for estimating the volume density ($V_v$), that is neurons (*), neuropil (N), and capillaries (arrows). Toluidine blue. Scale bar: 20 μm.

method (Gundersen, 1988) in the reference sections used for neuron numerical density estimation, that is on an average 15, 17, 24, and 25 sets of sections were used for newborn, young, adult, and aged pacas, respectively. Nucleoli were sampled using one 2-μm and one 0.5-μm thick sections in a physical disector. The height of the smaller physical disector was 2 μm. For mononucleate neurons on average 107 cells were measured for newborn and young, and 103 cells for adult and aged pacas. For binucleate neurons on average 102 cells were measured for newborn and young, and 103 cells for adult and aged pacas.

The following formula was used to estimate neuronal size:

$\bar{v}_N := \Sigma(4\pi/3)\cdot\bar{l}_n^3$, where: $\bar{l}_n^3$ is the mean cubed distance from a cell central point (nucleolus) to cell boundaries. Distances from a cell central point to cell boundaries were measured with a special ruler divided into classes of different length, on a flat computer monitor on which a test-system, constituted of sine-weighted lines to the vertical axis, was superimposed to increase the efficiency of the procedure (Sorensen, 1991; Tandrup, 1993).

## The Precision of Stereological Estimates

The precision of stereological estimates, that is SCG volume, total number neurons and volume density, was assessed by estimating their coefficients of error (CEs). Since each ganglion produced from eight to fourteen half-slabs (or tissue blocks) (Fig. 2), the CEs for each half (or each tissue block) were estimated according to Gundersen et al. (1999) and combined to give the total estimates ($CE_{total}$) using Eq. (4) of Dorph-Petersen et al. (2004) and Dorph-Petersen et al. (2008), who used a design for the human mediodorsal thalamic nucleus (MD) and for the human lateral geniculate nucleus (LGN), respectively, which were also split into two blocks before cutting:

$$CE_{total} := \frac{\sqrt{(CE_{1.1}\cdot Est_{1.1})^2 + \cdots + (CE_{5.2}\cdot Est_{5.2})^2}}{Est_{1.1} + \cdots + Est_{5.2}}$$

where $Est_{1.1}$ and $Est_{5.2}$ are the relevant estimates for half-slabs 1.1 and 5.2, which were represented in Figure 2.

## Statistical Analysis

Normally distributed data was tested using one-way ANOVA through Minitab 15® (2007). Normal distribution was ensured using Anderson-Darling's test and equality of variances was tested by Levene's test. When significant intergroup differences ($P < 0.05$) were noted Tukey's test was applied for multiple comparisons. Results are shown as mean (CVobs), where observed coefficient of variation (CVobs) equals SD/mean. In addition, some parameters, that is total number of mono and binucleate neurons, were also analyzed using Pearson's product-moment correlation to test the interrelation between animal body weight and the total number of neurons, ganglion volume and the total number of neurons, and between ganglion volume and animal body weight (Kutner et al., 2005). The correlation coefficient (ρ) varies from −1 to +1. When $\rho < 0.3$ there is no correlation between variables, $\rho = 0.3$–$0.5$ lower correlation, $\rho = 0.5$–$0.7$ medium correlation, and $\rho > 0.7$ higher correlation (Kutner et al., 2005).

# RESULTS

## Anatomy

In all pacas and independently of age, the SCG was roughly elliptical and was located in the most cranial part of the neck. Dorsally, the ganglion was in contact with the vagus nerve and ventrally, it was close to the occipital artery. The caudal pole of the ganglion continued into the cervical sympathetic trunk. In newborn pacas, SCG width, length, and thickness were 2.21 mm (0.06), 4.50 mm (0.30), and 1.26 mm (0.19), respectively. In young pacas, the values were: 1.98 mm (0.24), 5.37 mm (0.06), and 1.31 mm (0.35). For adult pacas, figures were: 3.17 mm (0.18), 7.36 mm (0.12), and 1.59 mm (0.09), and for aged pacas figures were 2.86 mm (0.13), 7.66 mm (0.15), and 2.20 mm (0.36). Differences amongst groups were significant ($P = 0.007$) for ganglion width

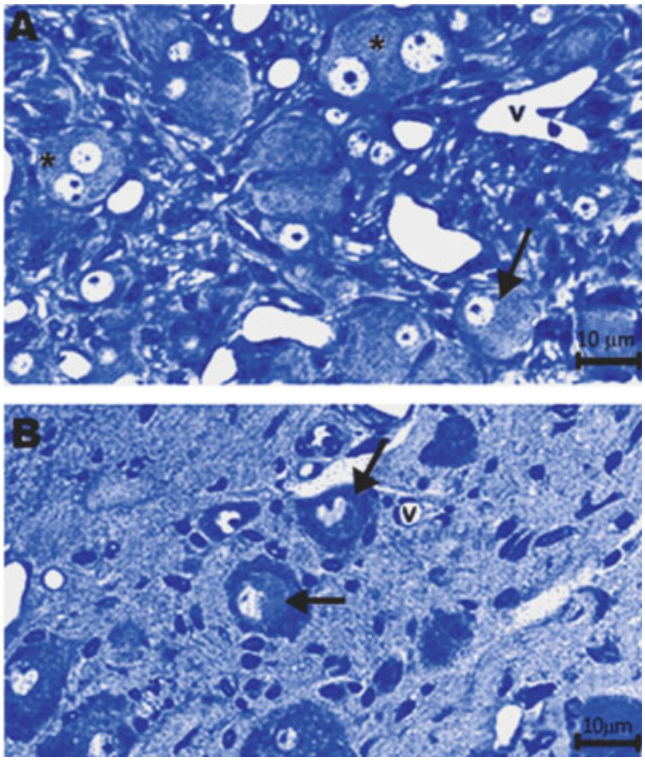


Fig. 5. Structure of the superior cervical ganglion of a newborn (**A**) and aged paca (**B**) in semi-thin sections (2 μm) at the same magnification. The newborn animal shows a higher neuronal profile density of mono (arrow) and binucleate neurons (*) separated by vessels which are also more densely distributed (v). However, in aged pacas both nerve cell bodies (arrows) and vessels (v) are more distant since they are separated by large spaces mainly occupied by non-neuronal tissue. Toluidine blue. Scale bar: 10 μm.

and length but they were not significant for ganglion thickness ($P = 0.8$).

## Microstructure

In semi-thin sections, the ganglion consisted of clusters of neurons separated by nerve fibers, blood vessels, and prominent septa of connective tissue. Ganglion neuron profiles were circular or, more commonly, oval shaped. In mononucleate neurons some nuclei were located in the center of the perikaryon, while the majority was eccentric, but none placed at the periphery of the neuronal profile. On the other hand, in binucleate neurons the nuclei occupied the two poles of the cell having a very distinct and defined position within the cell (Fig. 5).

## Stereology

***Numerical density of mononucleate and binucleate neurons: $N_v$(mononuc, SCG) and $N_v$(binuc, SCG).*** The numerical density of mononucleate neurons was 6,710 $mm^{-3}$ (0.28) in newborn, 6,872 $mm^{-3}$ (0.40) in young, 5,350 $mm^{-3}$ (0.47) in adult, and 5,145 $mm^{-3}$ (0.30) in aged pacas. Nonsignificant differences were noted amongst groups ($P = 0.235$).

The numerical density of binucleate neurons was 3,450 $mm^{-3}$ (0.23) in newborn, 4,600 $mm^{-3}$ (0.34) in young, 2,990 $mm^{-3}$ (0.37) in adult, and 2,160 $mm^{-3}$ (0.33) in aged pacas. Differences amongst groups were significant ($P = 0.018$).

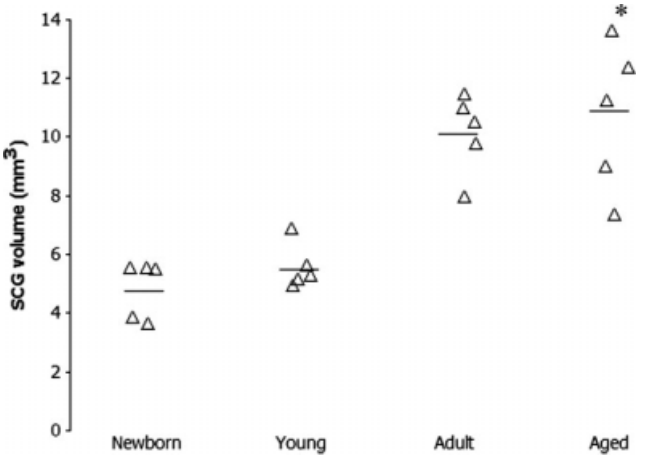


Fig. 6. SCG volume in pacas during post natal development. There were significant differences amongst age groups ($P = 0.0001$*). Triangles indicate individual values and horizontal bars show group means.

## Volume of Ganglion: V(SCG)

SCG volume was 4.52 $mm^3$ (0.20) in newborn, 5.57 $mm^3$ (0.17) in young, 10.1 $mm^3$ (0.17) in adult, and 11.5 $mm^3$ (0.21) in aged pacas. Differences amongst groups were significant ($P = 0.0001$) (Fig. 6). The coefficient of error of the Cavalieri estimate was 0.08 for newborn, 0.08 for young, 0.09 for adult, and 0.10 for aged pacas.

***Total number of mononucleate and binucleate neurons: N(mononuc, SCG) and N(binuc, SCG).*** The total number of mononucleate neurons was 30,300 (0.20) in newborn, 38,300 (0.22) in young, 54,200 (0.19) in adult, and 59,200 (0.11) in aged pacas. Differences amongst groups were significant ($P = 0.006$) (Fig. 7A). The total number of binucleate neurons was 15,600 (0.24) in newborn, 25,600 (0.27) in young, 30,300 (0.23) in adult, and 24,800 (0.26) in aged pacas. Differences amongst groups did not attain statistical significance ($P = 0.08$) (Fig. 7B). For mononucleate neurons CE(N) was 0.08 for newborn, 0.08 for young, 0.07 for adult, and 0.06 for aged pacas. For binucleate neurons CE(N) was 0.08 for newborn, 0.09 for young, 0.07 for adult, and 0.08 for aged pacas.

***Volume density of neurons: $V_v$ (neurons, SCG) and of the non-neuronal tissue: neuropil ($V_v$(neuropil, SCG)) and capillaries ($V_v$(cap, SCG)).*** The volume density of neurons was: 0.32 (0.15) in newborn, 0.23 (0.27) in young, 0.20 (0.35) in adult, and 0.19 (0.27) in aged pacas. Differences amongst groups were significant ($P = 0.002$). The volume density of the neuropil was: 0.60 (0.14) in newborn, 0.71 (0.26) in young, 0.76 (0.20) in adult, and 0.79 (0.17) in aged pacas. Differences amongst groups were significant ($P = 0.002$). The volume density of the capillaries was: 0.08 (0.14) in newborn, 0.06 (0.26) in young, 0.04 (0.21) in adult, and 0.02 (0.17) in aged pacas. Differences amongst groups were

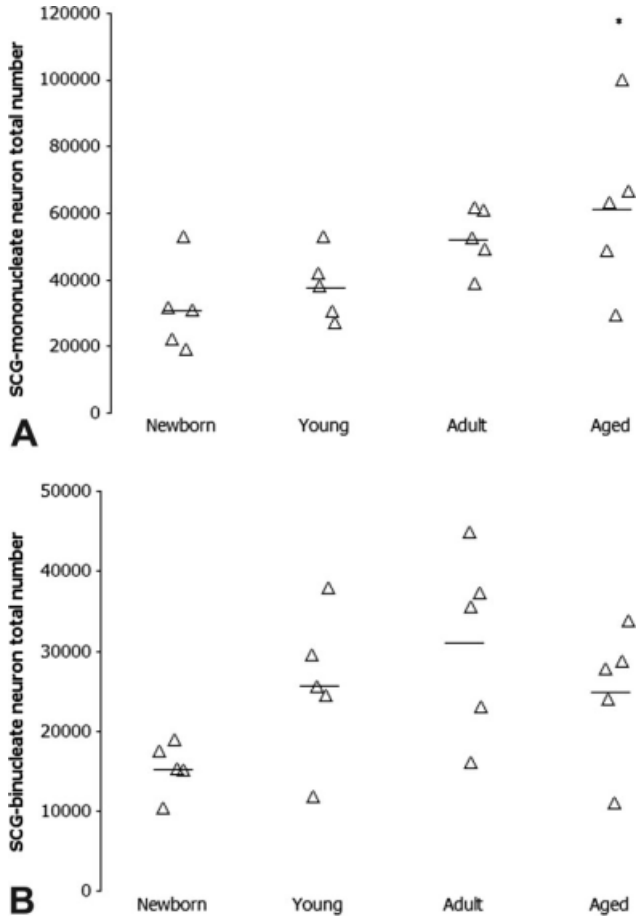


Fig. 7. Total number of mononucleate (**A**) and binucleate (**B**) SCG neurons in pacas. Intergroup differences were significant for mononucleate neurons ($P = 0.006$*) while no differences were detected for binucleate neurons ($P = 0.08$). Triangles indicate individual values and horizontal bars show group means.

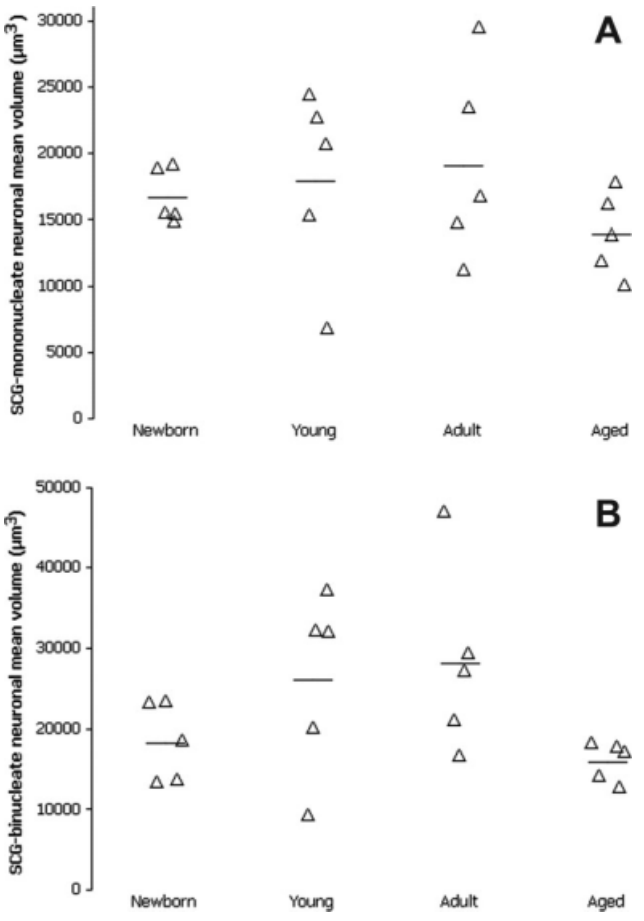


Fig. 8. Mean perikaryal volume of mononucleate (**A**) and binucleate (**B**) SCG neurons in pacas. Differences amongst groups did not attain significance for either mononucleate ($P = 0.489$) or binucleate neurons ($P = 0.107$). Triangles indicate individual values and horizontal bars show group means.

significant ($P = 0.001$). For neurons CE(Vv) was 0.06 for newborn, 0.07 for young, 0.08 for adult, and 0.07 for aged pacas. As to neuropil CE(Vv) was 0.06 for newborn, 0.07 for young, 0.07 for adult, and 0.07 for aged pacas, and for capillaries, CE(Vv) was 0.04 for newborn, 0.07 for young, 0.08 for adult, and 0.07 for aged pacas.

***Mean volume of mononucleate and binucleate neurons: $\bar{v}_N$(mononuc, SCG) and $\bar{v}_N$(binuc, SCG).*** The mean perikaryal volume of mononucleate neurons was 16,700 $\mu m^3$ (0.13) in newborn, 17,900 $\mu m^3$ (0.54) in young, 19,100 $\mu m^3$ (0.49) in adult, and 13,900 $\mu m^3$ (0.15) in aged pacas (Fig. 8A). For binucleate neurons figures were 18,300 $\mu m^3$ (0.26) in newborn, 26,000 $\mu m^3$ (0.57) in young, 28,100 $\mu m^3$ (0.58) in adult, and 15,800 $\mu m^3$ (0.18) in aged pacas (Figs. 8B and 9). Differences amongst groups were not significant for either mononucleate ($P = 0.489$) or binucleate ($P = 0.107$) neurons.

***Total volume of neurons: V(neurons, SCG) and of the non-neuronal tissue: neuropil (V(neuropil, SCG)) and capillaries (V(cap, SCG)).*** The total volume occupied by neurons in the SCG was 1.45 $mm^3$ (0.36) in newborn, 1.28 $mm^3$ (0.47) in young, 2.03 $mm^3$ (0.40) in adult, and 2.18 $mm^3$ (0.44) in aged pacas. Differences amongst groups were significant ($P = 0.03$). The total volume of the neuropil was: 2.71 $mm^3$ (0.14) in newborn, 3.96 $mm^3$ (0.27) in young, 7.70 $mm^3$ (0.14) in adult, and 9.09 $mm^3$ (0.17) in aged pacas. Differences amongst groups were significant ($P = 0.0002$). The total volume occupied by capillaries was: 0.36 $mm^3$ (0.14) in newborn, 0.33 $mm^3$ (0.16) in young, 0.41 $mm^3$ (0.11) in adult, and 0.23 $mm^3$ (0.27) in aged pacas. Differences amongst groups were significant ($P = 0.013$).

***Correlation between variables.*** High-intensity correlations were found between the total number of mononucleate neurons N(mononuc, SCG) and the volume of ganglion V(SCG) ($\rho = 0.81$) and between the volume of ganglion V(SCG) and animal body weight ($\rho = 0.85$). However, medium-intensity ($\rho = 0.63$; $\rho = 0.60$) and low-intensity ($\rho = 0.37$) correlations were observed between the total number of mononucleate neurons N(mononuc, SCG) and animal body weight, between the total number of binucleate neurons N(binuc, SCG) and the volume of ganglion V(SCG), and between the total

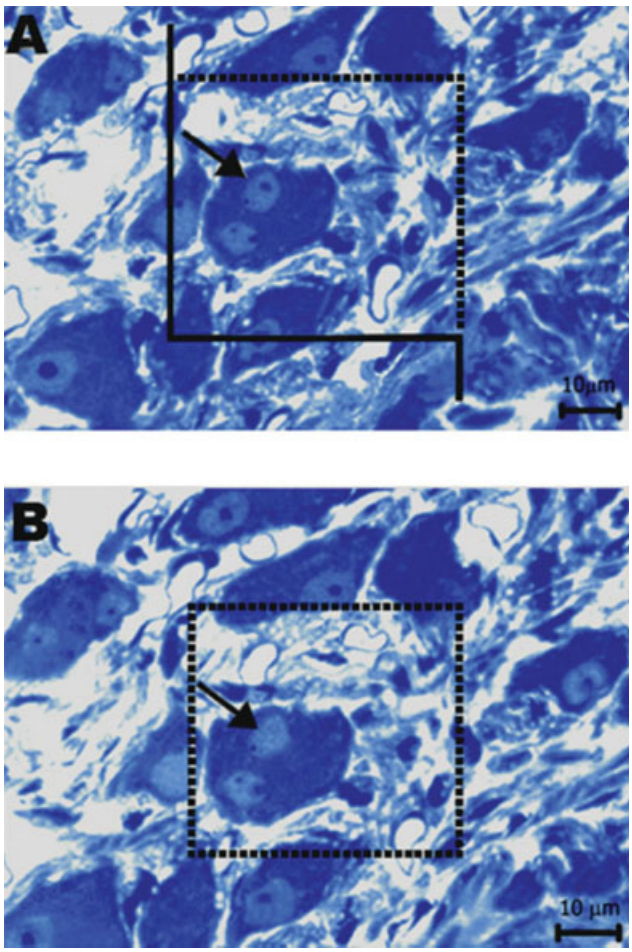


Fig. 9. An example of a disector-sampled neuron for volume estimation using the nucleator. The reference section (**A**) and look-up 1 section (**B**) are separated by a height of 2 μm. In (**A**) the arrow shows a neuron nucleus profile whose nucleolus appears in the reference section but is no longer in the look-up 1 section (arrow) and was, therefore, sampled for neuron volume estimate. Toluidine blue. Scale bar: 10 μm.

number of binucleate neurons N(binuc, SCG) and animal body weight, respectively.

## DISCUSSION

The main age-dependent findings of this study were: (i) a 154% increase in the SCG volume, (ii) a 95% increase in the total number of mononucleate SCG neurons, and (iii) a 50% increase in the total volume of SCG neurons.

### Anatomy

Postnatal development comprises both maturation and ageing and several organic adaptive mechanisms occur (Finch, 1993; Vega et al., 1993). For instance, the 70% and 920% increases in ganglion length and body size, respectively, were attributed to a combination of maturation and ageing processes. These findings are in agreement with previous studies conducted on the SCG from other medium-sized (hamsters, guinea pigs) (Purves et al., 1986b) and large rodents (capybaras) (Ribeiro et al., 2004 and Ribeiro, 2006). The former showed that an allometrical pattern exists between either body weight and ganglion size or body weight and total number of ganglion neurons applying 2D morphometric methods, although we used 3D design-based stereological methods (Ribeiro et al., 2004 and Ribeiro, 2006).

### Microstructure

Using semi-thin section light microscopy, all ganglia were enveloped by a connective capsule which sent septa of connective tissue inside the SCG, dividing it into several ganglion units. This general pattern was also found in all pacas, irrespective of age, and this is in line with previous qualitative studies that focused on the sympathetic ganglia of several large mammals such as dogs, horses, cats (Ribeiro et al., 2002; Gagliardo et al., 2003; Fioretto et al., 2007), rabbits (Sasahara et al., 2003) and capybaras (Ribeiro et al., 2004; Ribeiro, 2006).

### Stereology

Postnatal development exerted no effect on the numerical density of mononucleate neurons, which differs from Ribeiro (2006) who reported a 26% decrease in the numerical density of mononucleate SCG neurons in capybaras during maturation. Age-induced neuronal density decreases have also been reported by Purves et al. (1986b) (using 2D morphometry), Ribeiro et al. (2004), Gagliardo et al. (2005), and Ribeiro (2006) for several sympathetic ganglia using 3D design-based stereological methods.

As with previous studies (Ribeiro et al., 2004; Gagliardo et al., 2005; Ribeiro, 2006) maturation and ageing in pacas were marked by a 154% increase in ganglion volume. Ganglion hypertrophy seems to be a common adaptive mechanism during postnatal development and this can be seen in most autonomic ganglia from medium-sized to large mammals (Miolan and Niel, 1996; Fioretto et al., 2007). However, it should be stressed that the larger proportion of ganglia volume is occupied by the non-neuronal tissue, that is neuropil and blood vessels, and differences in ganglion volume reflect, in part, a variation in the total volume of the nervous tissue and, in part, a variation of vascular and neuropil total volumes. The nervous tissue volume, that is SCG neurons, increased by 50% during the post-natal phase. Paradoxically, the fractional volume (ratio) occupied by the same SCG neurons decreased by 41% during the same period. This phenomenon confirms that purely ratio-based conclusions are generally misleading due to the reference trap, which happens when there is no knowledge of the organ volume (reference volume) (Braendgaard and Gundersen, 1986; Hunziker and Cruz-Orive, 1986; Cruz-Orive, 1994; Nyengaard, 1999; Mayhew, 2008). The non-neuronal tissue amounted, however, to a larger fraction of the SCG volume, that is 68% in newborn, 77% in young, 80% in adult, and 81% in aged pacas. For instance, neuropil increased by 235% during post-natal development whereas vascular tissue decreased by 37% in the same period.

The main finding of this study was a 95% age-dependent increase in the total number of mononucleate SCG neurons, though no changes were observed in the total number of binucleate SCG neurons. By contrast, Ribeiro (2006) reported a 23% decrease in the total number of binucleate SCG neurons in capybaras during maturation. Again, a wrong conclusion could be drawn if it was based only on ratios (reference trap), compare that is a 37% decrease in the numerical density of binucleate SCG neurons had no effect on the total number of the same neurons. Generally speaking, the differences in the total number of ganglion neurons are related to body weight and organ weight ranges, the largest species or organs having the largest number of neurons, though they are obviously not proportional to body weight variations. Indeed, Mayhew (1991) using a direct design-based stereological number estimator, that is the physical fractionator, showed that the weight of the mammalian cerebellum affords a satisfactory way of predicting the total number of Purkinje cells. Further, Gagliardo et al. (2005) reported that a dog's body weight allowed an accurate prediction of the total number of caudal mesenteric ganglion (CMG) neurons which increased with maturity and ageing. Along the same lines, in our study a high-intensity correlation has been found between the number of mononucleate neurons and ganglion volume, that is the larger the SCG the higher the number of mononucleate neurons.

In the central nervous system (CNS), the most frequently reported age-related changes are neocortical neuron loss, atrophy of remaining neurons (Esiri, 2007), hypertrophy, reduction in white matter and in the mean volume of Purkinje cell body and losses of both Purkinje and granular cells in the anterior lobe of cerebellum and of myelinated fibers in the human brain (Tang and Nyengaard, 1997; Cabello et al., 2002; Andersen et al., 2003; Marner et al., 2003; Pakkenberg et al., 2003). Nevertheless, these claims are controversial because there are related differences between various components of the nervous system and amongst animal species (Finch, 1993; Vega et al., 1993). Using design-based stereological methods, Farel (2003) reported that the increase in the number of neurons in the dorsal root ganglia (DRG) of rats was not associated with possible neurogenesis, but perhaps with a late maturation or incomplete differentiation. By the same token, a larger number of hypogastric ganglion neurons was reported by Warburton and Santer (1997) in rats of 24 months compared with rats of 4 months as well as in the DRG of 80-day-old rats compared with 11-day-old rats, by Popken and Farel (1997).

In addition, there were no changes in neuron size during postnatal development. Along similar lines, Ribeiro (2006) also reported no changes in the volume of capybara's SCG neurons during postnatal development. On the contrary, neuron volume increased by 217% in the dog's caudal mesenteric ganglion during maturation and ageing (Gagliardo et al., 2005). All quoted authors used local design-based stereological volume estimators. Although age-induced neuronal hypertrophy is widely known in some parts of the CNS (Cabello et al., 2002) the chances are that other adaptive mechanisms may coexist in the autonomic nervous system to guarantee functional homeostasis.

## Conclusions and Remarks for Further Studies

Further investigation should be conducted, using either proliferation markers such as: bromodeoxyuridine (Brd-U), Brd-U/PCNA, Thymidine, and KI-67 or apoptosis markers (caspases), to shed light on what really happens to binucleate neurons during postnatal development. By the same token, there is a need for mechanistic studies focusing on the functional role played by binucleate neurons.

## ACKNOWLEDGMENTS

The authors thank the reviewers for very positive and constructive comments, which helped us improve this MS substantially.

## LITERATURE CITED

Andersen BB, Gundersen HJG, Pakkenberg B. 2003. Aging of the human cerebellum: a stereological study. J Comp Neurol 466: 356–365.

Baddeley AJ, Gundersen HJG, Cruz-Orive LM. 1986. Estimation of surface area from vertical sections. J Microscopy 142:259–276.

Braendgaard H, Gundersen HJG. 1986. The impact of recent stereological advances on quantitative studies of the nervous system. J Neurosci Method 18:39–78.

Cabello CR, Thune JJ, Pakkenberg H, Pakkenberg B. 2002. Ageing of substantia nigra in humans: cell loss may be compensated by hypertrophy. Neuropathol Appl Neurobiol 28:283–229.

Cruz-Orive LM. 1994. Toward a more objective biology. Neurobiol Aging 15:377–378.

Dorph-Petersen KA, Pierri JN, Sun Z, Sampson AR, Lewis DA. 2004. Stereological analysis of the mediodorsal thalamic nucleus in schizophrenia: volume, neuron number, and cell types. J Comparative Neurol 472:449–462.

Dorph-Petersen KA, Caric D, Saghafi R, Zhang W, Sampson AR, Lewis DA. 2009. Volume and neuron number of the lateral geniculate nucleus in schizophrenia and mood disorders. Acta Neuropathol 117:369–384.

Erankö L. 1972. Postnatal development of histochemically demonstrable catecholamines in the superior cervical ganglion of the rat. Histochem J 4:225–236.

Esiri M. 2007. Ageing and the brain. J Pathol 211:181–187.

Eskild-Jensen A, Paulsen LF, Wogensen L, Olesen P, Pedersen L, Frøkiaer J, Nyengaard JR. 2007. AT1 receptor blockade prevents interstitial and glomerular apoptosis but not fibrosis in pigs with neonatal induced partial unilateral ureteral obstruction. Am J Physiol Renal Physiol 292:F1771–F1781.

Farel PB. 2003. Late differentiation contributes to the apparent increase in sensory neuron number in juvenile rat. Dev Brain Res 144:91–98.

Finch CE. 1993. Neuron atrophy during aging: programmed or sporadic? Trends Neurosci 6:104–110.

Fioretto ET, Abreu RN, Castro MFS, Guidi WL, Ribeiro AACM. 2007. Macro and microstructure of the superior cervical ganglion in dogs, cats and horses during maturation. Cells Tissues Organs 186:129–140.

Gagliardo KM, Silva RA, Guidi WL, Ribeiro AACM. 2003. Macro and microestructural organization of the dog's caudal mesenteric ganglion complex (canis familiaris). Anatomia Histologia Embryologia 32:236–243.

Gagliardo KM, Balieiro JCC, Souza RR, Ribeiro AACM. 2005. Postnatal-related changes in the size and total number of neurons in the caudal mesenteric ganglion of dogs: total number of neurons can be predicted from body weight and ganglion volume. Anat Rec 286:917–929.

Gundersen HJG. 1977. Notes of the estimation of the numerical density of arbitrary profiles: the edge effect. J Microsc 111: 219–223.

Gundersen HJG. 1986. Stereology of arbitrary particles. A review of unbiased number and size estimators and presentation of some new ones, in memory of William R. Thompson. J Microsc 143: 3–45.

Gundersen HJG. 1988. The nucleator. J Microsc 151:3–21.

Gundersen HJG, Jensen EB, Kiêu K, Nielsen J. 1999. The efficiency of systematic sampling in Stereology: reconsidered. J Microsc 193:199–211.

Hunziker EB, Cruz-Orive LM. 1986. Consistent and efficient delineation of reference spaces for light microscopical stereology using a laser microbeam system. J Microsc 142:95–99.

Kutner MH, Nachtsheim CJ, Neter J, Li W. 2005. Applied linear statistical models. 5th ed. New York: McGraw-Hill Irwin. p 1396.

Lima AR, Nyengaard JRN, Jorge AAL, Balieiro JCC, Peixoto C, Fioretto ET, Ambrósio CE, Miglino MA, Zatz M, Ribeiro AACM. 2007. Muscular dystrophy-related quantitative and chemical changes in adenohypophysis GH-cells in Golden Retrievers. Growth Hormone IGF Res 17:480–491.

Mayhew TM. 1991. Accurate prediction of Purkinje cell number from cerebellar weight can be achieved with the fractionator. J Comp Neurol 308:162–168.

Mayhew TM. 2008. Taking tissue samples from the placenta: an illustration of principles and strategies. Placenta 29:1–14.

Marner L, Nyengaard JR, Tang Y, Pakkenberg B. 2003. Marked loss of myelinated nerve fibers in the Human Brain with Age. J Comp Neurol 462:144–152.

Minitab (v.15). 2007. Minitab reference manual. Minitab Inc. State College PA, USA.

Miolan J, Niel J. 1996. The mammalian sympathetic prevertebral ganglia: integrative properties and role in the nervous control of digestive tract motility. J Autonomic Nervous Syst 58:125–138.

Nowak R. 1999. Walker's mammals of the World. Vol. 2. Baltimore and London: The Johns Hopkins University Press.

Nyengaard JR. 1999. Stereologic methods and their application in kidney research. J Am Soc Nephrol 10:1100–1123.

Pakkenberg B, Pelvig D, Marner L, Bundgaard MJ, Gundersen HJG, Nyengaard JR, Regeur L. 2003. Aging and the human neocortex. Exp Gerontol 38:95–99.

Popken GJ, Farel PB. 1997. Sensory neuron number in the neonatal and adult rats estimated by means of the stereologic and profile-based methods. J Comp Neurol 386:8–15.

Purves D, Rubin E, Snider WD, Lichtman J. 1986b. Relation of animal size to convergence, divergence, and neuronal number in peripheral sympathetic pathways. J Neurosci 6:158–163.

Ribeiro AACM, Elias CF, Liberti EA, Guidi WL, De Souza RR. 2002. Structure and ultrastructure of the celiac-mesenteric ganglion complex in the domestic dog (*Canis familiaris*). Anat Histol Embryol 31:344–349.

Ribeiro AACM, Davis C, Gabella G. 2004. Estimate of size and total number of neurons in superior cervical ganglion of rat, capybara and horse. Anat Embryol 208:367–380.

Ribeiro AACM. 2006. Size and number of binucleate and mononucleate superior cervical ganglion neurons in young capybaras. Anat Embryol (Berl) 211:607–617.

Rowe D, Honeycutt R. 2002. Phylogenetic relationships, ecological correlates, and molecular evolution within the Cavioidea (Mammalia, Rodentia). Mol Biol Evol 19:263–277.

Sasahara THC, Souza RR, Machado MRF, Silva RA, Guidi WL, Ribeiro AACM. 2003. Macro- and microstructural organization of the rabbit's celiac-mesenteric ganglion complex (Oryctolagus cuniculus). Ann Anat 185:441–448.

Scherle W. 1970. A simple method for volumetry of organs in quantitative stereology. Mikroskopie 26:57–60.

Sorensen FB. 1991. Stereological estimation of the mean and variance of nuclear volume from vertical sections J. Microsc 162:203–229.

Tandrup T. 1993. A method for unbiased and efficient estimation of number and mean volume of specified neuron subtypes in rat dorsal root ganglion. J Comp Neurol 329:269–276.

Tandrup T, Braendgaard H. 1994. Number and volume of rat dorsal root ganglion cells in acrylamide intoxication. J Neurocytol 23:242–248.

Tang Y, Nyengaard JR. 1997. A stereological method for estimating the total length and size of myelin fibers in human brain white matter. J Neurosci Method 73:193–200.

Vega JA, Calzada B, Del Valle ME. 1993. Age-related in the mammalian autonomic and sensoryganglia. In: Amenta F, editor. Aging of the autonomic nervous system. London: CRC Press. p 31–61.

Warburton AL, Santer RM. 1997. The hypogastric ant thirteenth thoracic ganglia of the rat: effects of age on the neurons and their extracellular environment. J Anat 190:115–124.

Wilson DE, Reeder DM. 2005. Mammal species of the world: a taxonomic and geographic reference. 3rd ed. Baltimore, Maryland: Johns Hopkins University Press. p 2,142.